FREE INTERNET ROWING MODEL (FIRM)

EXAMPLES: Quad Sculls

March 25, 2015

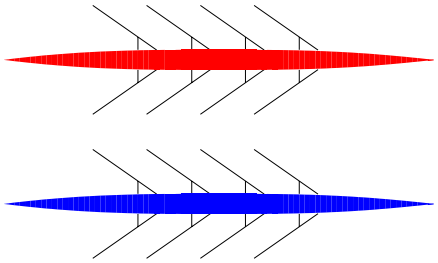

FIRM IS RESEARCH CODE!

Please check all estimates generated by the program against experimental results before committing any time or funds to your project as no liability can be accepted by Cyberiad.

©2015 Cyberiad
All Rights Reserved

Contents

1 INTRODUCTION

Two quad scull examples are included in this version of FIRM. More will be added in future versions.

1.1 W4x: Women's Quadruple Scull

The on-water trial for this women's quad, "Aage", "Bibi", "Xena" and "Yoko", was conducted over 4 minutes on an early spring morning. Air and water temperatures were not recorded: they were estimated as 11°C and 11°C respectively. Measured values of rigging details, oar angles, gate normal forces, and their anthropometry were used as input to FIRM. Body angle regimes were not recorded but were estimated by the author using a complicated fitting process.

A tail wind of 1.55 ms^{-1} was assumed for this simulation.

Aage was previously used in the W1x and W2x examples; Xena was partnered with Aage in the W2x example. This crew had not been together for very long and the members had just returned to training after a lay-off.

Table 1: Summary of experimental results for this simulation: number of strokes, stroke rate, non-dimensional pull phase duration (t_p/t_s), minimum hull velocity (U_{min}), maximum hull velocity (U_{max}), and mean hull velocity ($\overline{U}$).

Item	Value
Nstrokes	26
Rate (spm)	35.930 ±0.280
t_p/t_s	0.489 ±0.009
U_{min} (ms^{-1})	4.119 ±0.082
U_{max} (ms^{-1})	6.317 ±0.090
$\overline{U}$ (ms^{-1})	5.316 ±0.088

Table 1 summarises the main quantities relating to the simulation for this crew. Values are given ± one standard deviation.

Table 2: Experimental oar-related values for this simulation: Minimum and maximum oar angles, and maximum gate normal force.

Name	Port Oar			Starboard Oar		
	Min. Angle (degrees)	Max. Angle (degrees)	Max. F_{Gn} (N)	Min. Angle (degrees)	Max. Angle (degrees)	Max. F_{Gn} (N)
Aage	-58.6±0.44	44.1±0.48	382.2±25.8	-62.2±0.27	43.3±0.37	424.3±16.2
Bibi	-65.9±0.50	44.7±0.54	310.7±27.7	-64.5±0.58	45.9±0.62	274.6±16.8
Xena	-61.4±0.44	43.2±0.68	299.8±32.8	-63.8±0.48	40.1±1.08	332.6±45.1
Yoko	-60.7±0.45	43.3±0.63	365.9±24.9	-64.1±0.48	41.0±0.50	437.0±27.4

Table 2 summarises the measured oar angles and gate normal forces for this simulation. Note that the standard deviations of the gate forces are quite high for this crew.

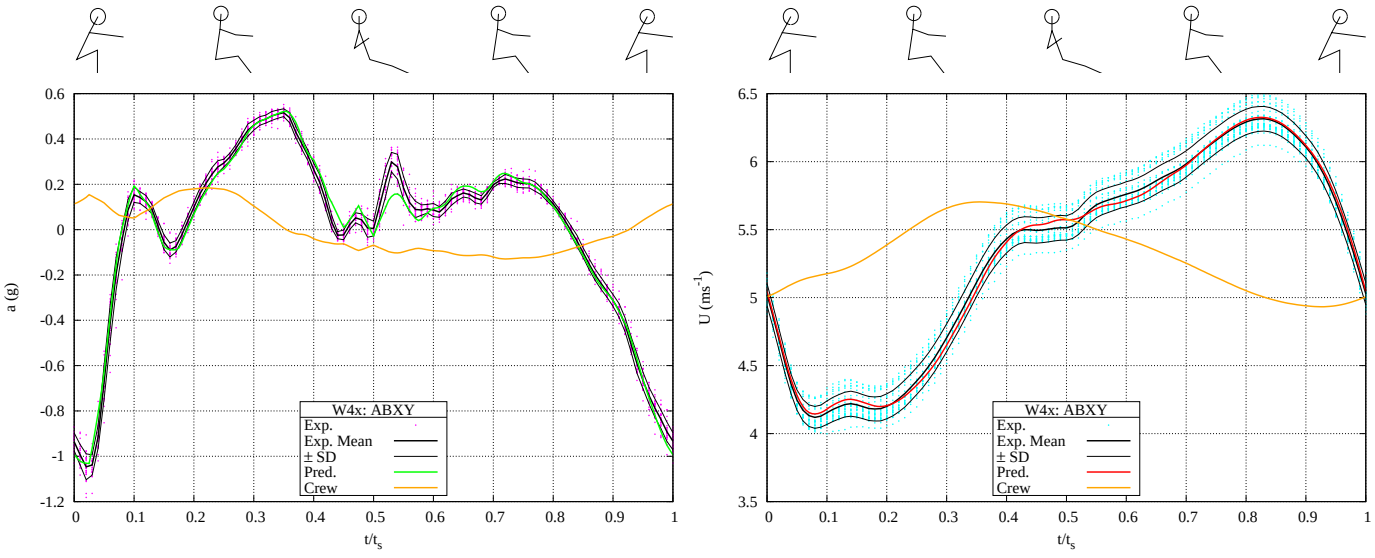

Figure 1: Hull propulsive acceleration and crew cg acceleration (left); hull velocity and crew cg velocity (right).

The hull propulsive acceleration is shown in the left panel of Fig. 1. Experimental data is shown as pink dots; the thick black curve is the mean of the measured values and the thin lines are one standard deviation (SD) either side of the mean curve. The green curve is FIRM's prediction.

Hull propulsive velocity and the speed of the crew CG is shown in the plot at the right of Fig. 1.

A tail wind of 1.55 ms^{-1} was used in this simulation to make the predicted mean velocity coincide with the measured mean. Increasing gate forces in Table 2 by 6.5% would produce the same mean hull velocity. These are relatively large adjustments, however, the standard deviations are of this order for some of the crew and less than the SD for Xena's gate forces. (See the plots of the measured gate forces below.)

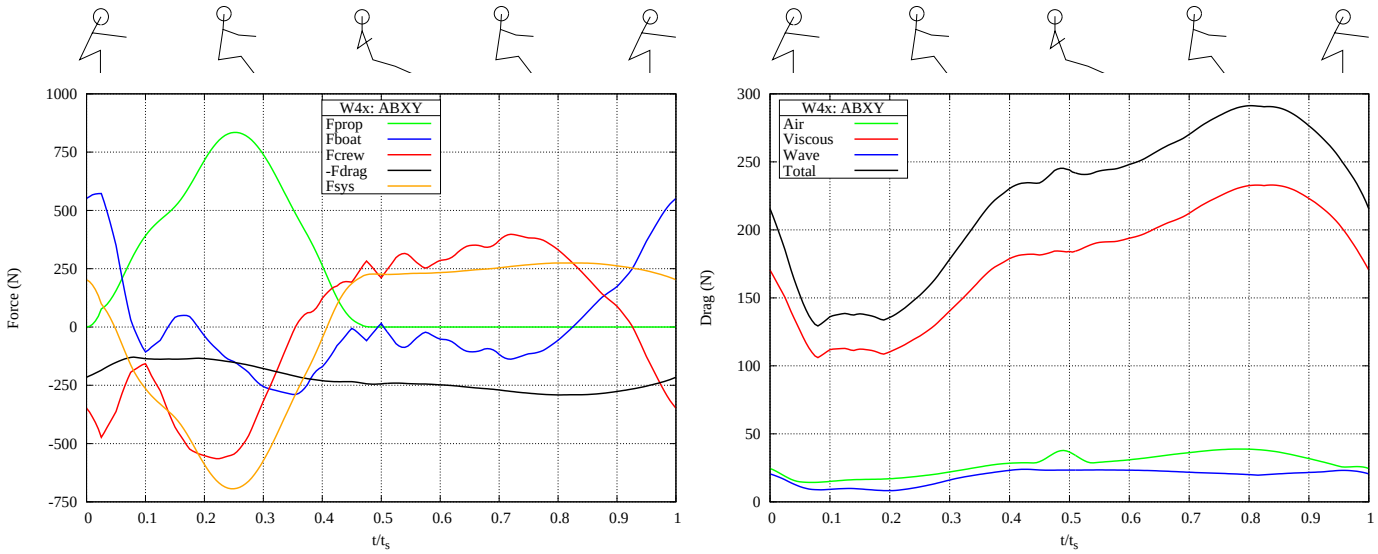

Figure 2: Equation of motion forces (left) and drag components (right).

The forces in the equations of motion are shown in the left panel of Fig. 2. Drag components during the stroke are in the panel at the right.

Oar angles are shown in the four plots at the left of Fig. 3; gate normal forces are shown in the four plots in the right column.

There is considerable scatter in the gate normal forces for the crew members. There is one stroke for Xena where it is clear that she missed the water with her starboard oar, or messed up the stroke in some other way. In a more rigorous analysis this stroke (and possibly the whole trial!) would be ignored, but we have left it in to show the difficulties that can arise with on-water measurements, and particulary in using simple averages without inspecting the details of the data set.

The solid curves were used as input to FIRM and were increased by about 6.5% to produce better agreement between FIRM predictions and measured values of the mean hull velocity.

Blade propulsive forces are shown in the four plots at the left of Fig. 4. Dynamic oar lever ratios shown in the right column of plots in Fig. 4 include the effect of variations in the location of the OBCP during the stroke. The different oarlever ratios for Bibi (Seat 2) are due to her use of a longer oarhandle in this trial.

Body angle regimes for two crew members are shown in the two parts of Fig. 5. The angles are the same for both crew members in this simulation.

Yawing moment lever arms and yawing moments are shown in the two parts of Fig. 6.

The OBCP trajectories in the yz-plane are shown in Fig. 7. For the purposes of this plot, the OBCP is assumed to be at the geometric centre of the blade when it is out of the water.

The OBCP is below the water from about $t/t_s = 0.01$ to $t/t_s \approx 0.49$. The latter value is the value entered in the main input file.

The OBCP trajectories in Fig. 8 have been plotted on the same side of the hull for clarity and comparison.

The OHCE x-wise velocities are shown in Fig. 9.

The x-wise seat velocities are shown in Fig. 10.

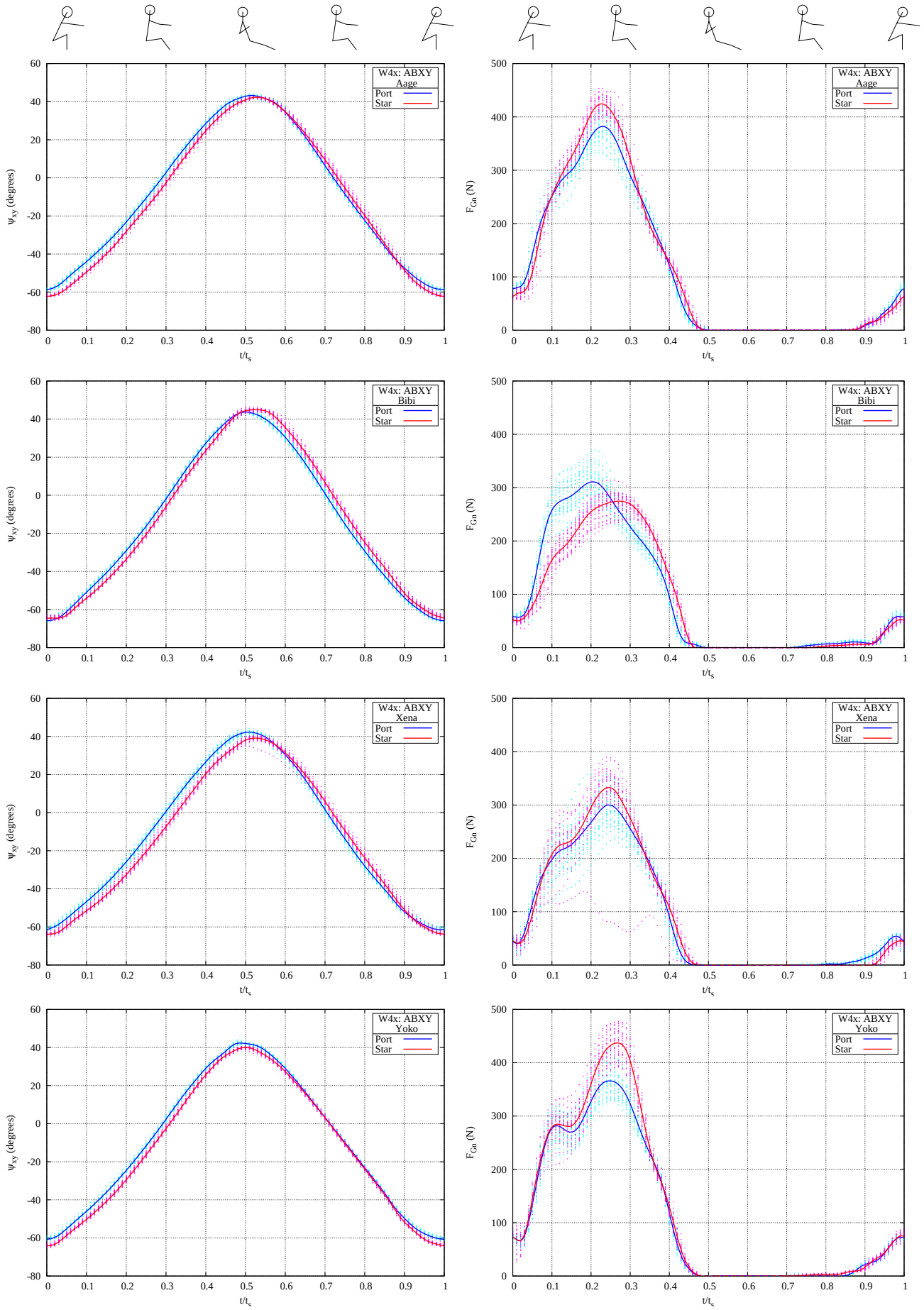

Figure 3: Oar azimuth angles Ψ_{xy} (left column) and gate normal forces F_{Gn} (right). Seat 1 (top row); Seat 2 (second row); Seat 3 (third row) and Seat 4 (bottom row).

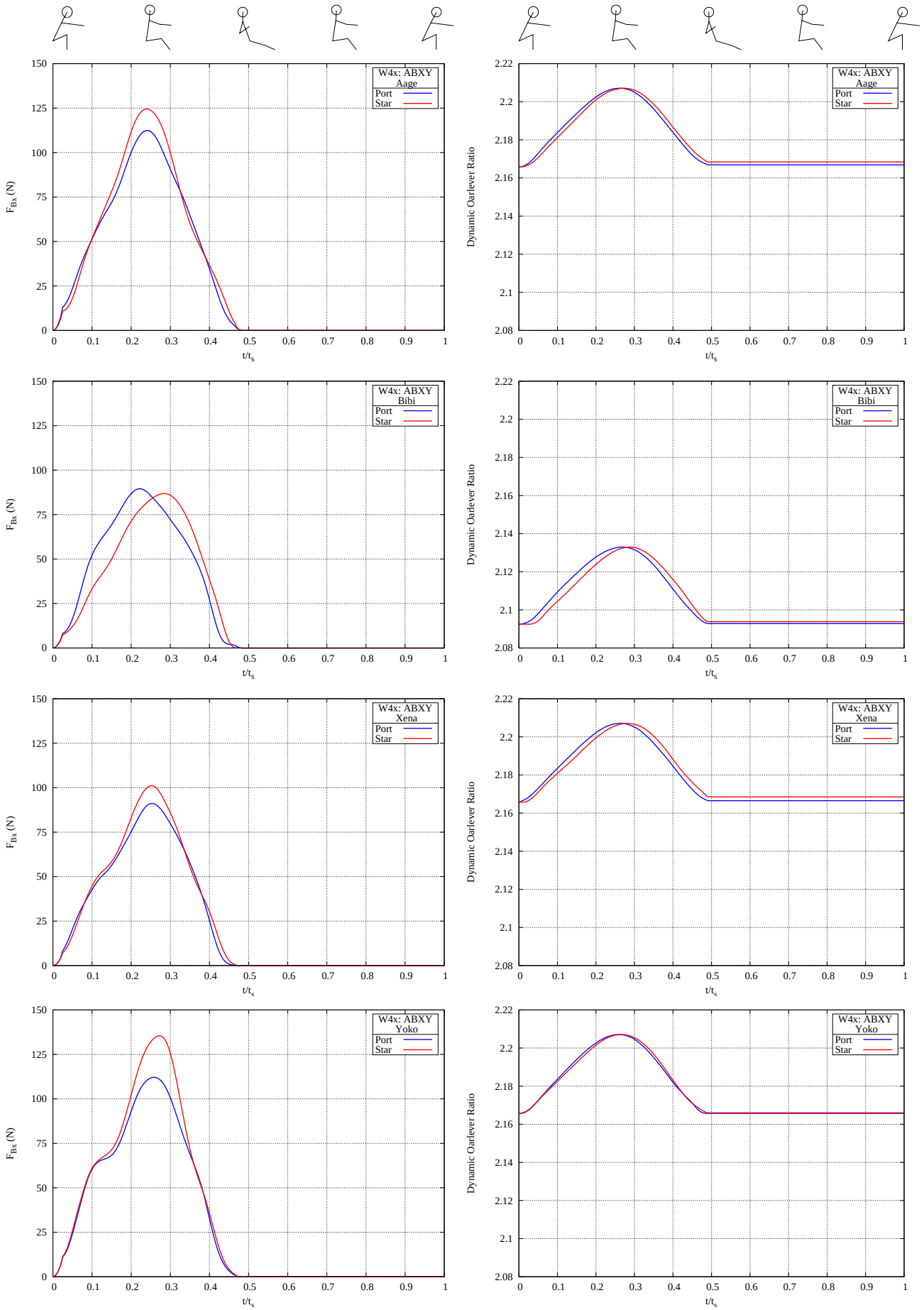

Figure 4: Blade propulsive forces F_{Bx} (left column) and dynamic oar lever ratios (right). Seat 1 (top row); Seat 2 (second row); Seat 3 (third row) and Seat 4 (bottom row).

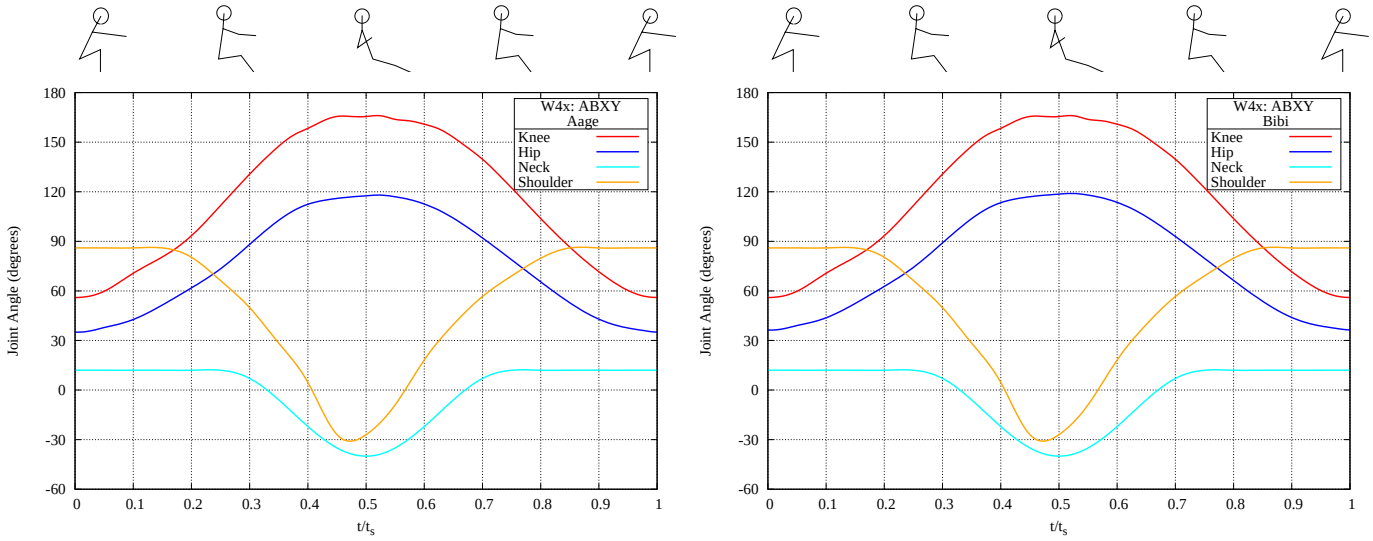

Figure 5: Joint angles: Seat 1 (left): Seat 2 (right).

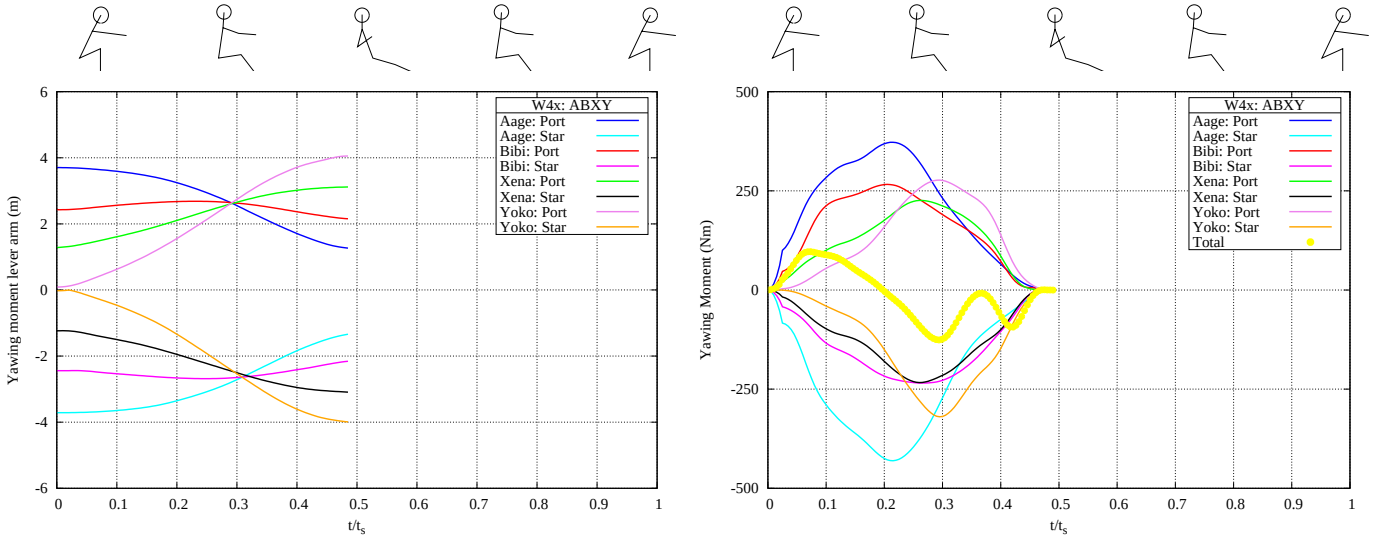

Figure 6: Yawing moment lever arms L_{yaw} (left); yawing moments M_{yaw} (right).

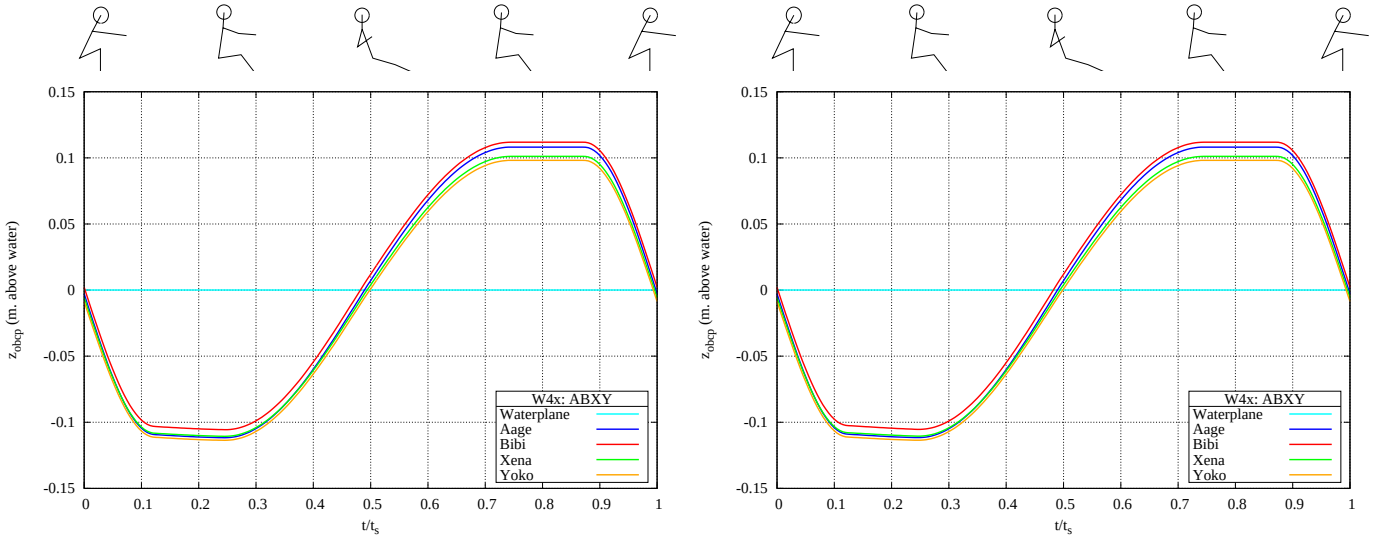

Figure 7: OBCP trajectories in the yz-plane: Port side (left); Starboard side (right).

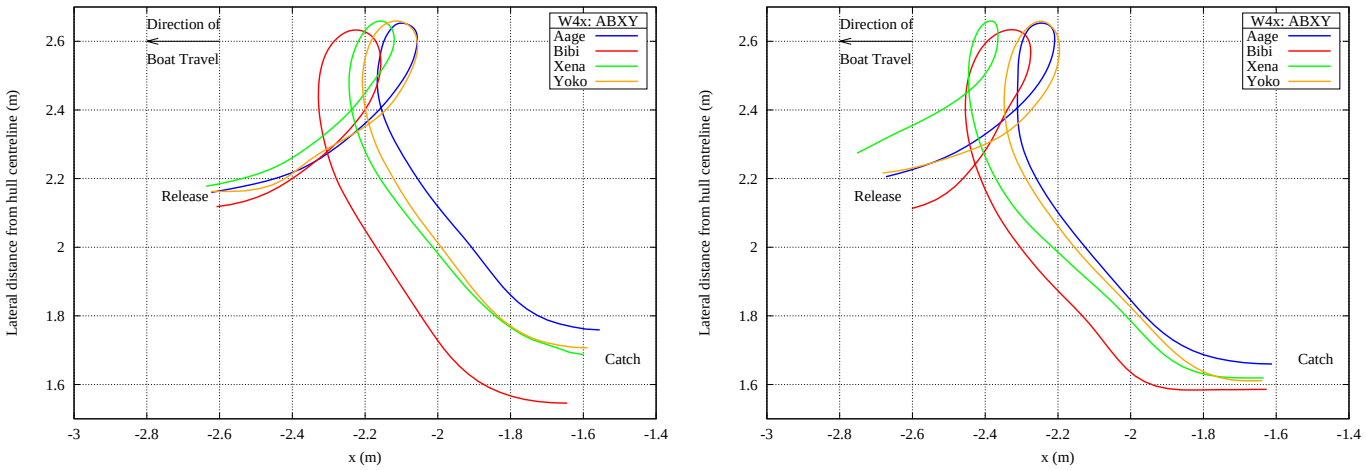

Figure 8: OBCP trajectories in the xy-plane: Port side (left); Starboard side (right).

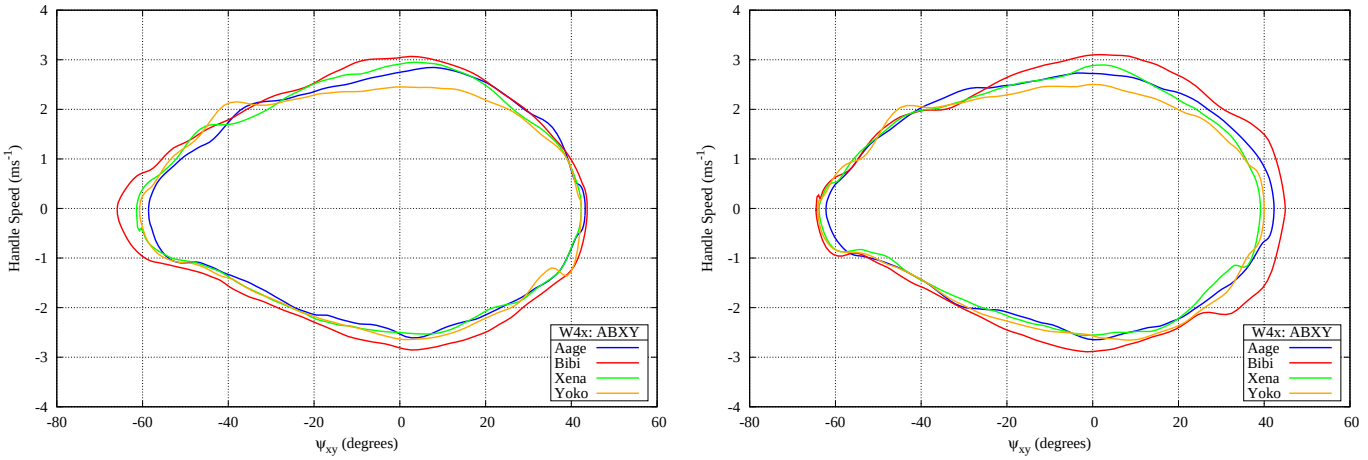

Figure 9: OHCE x-wise velocity: Port side (left); Starboard side (right).

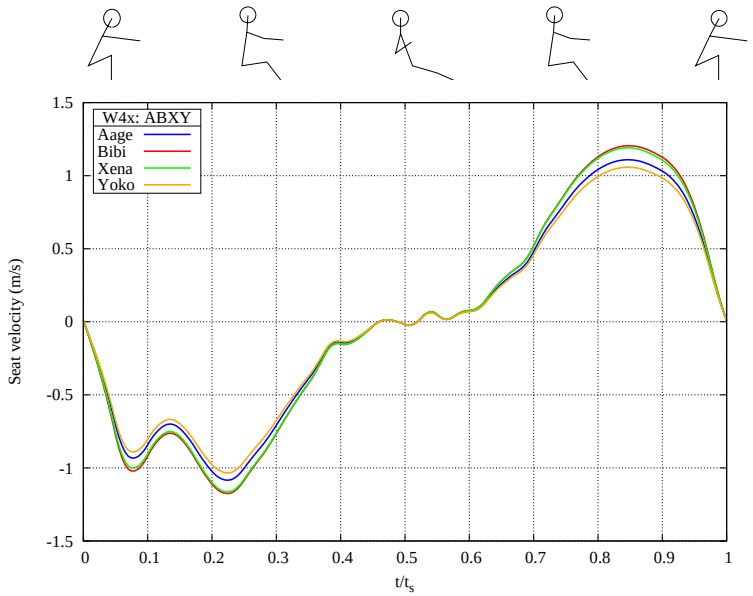

Figure 10: Seat x-wise velocities.

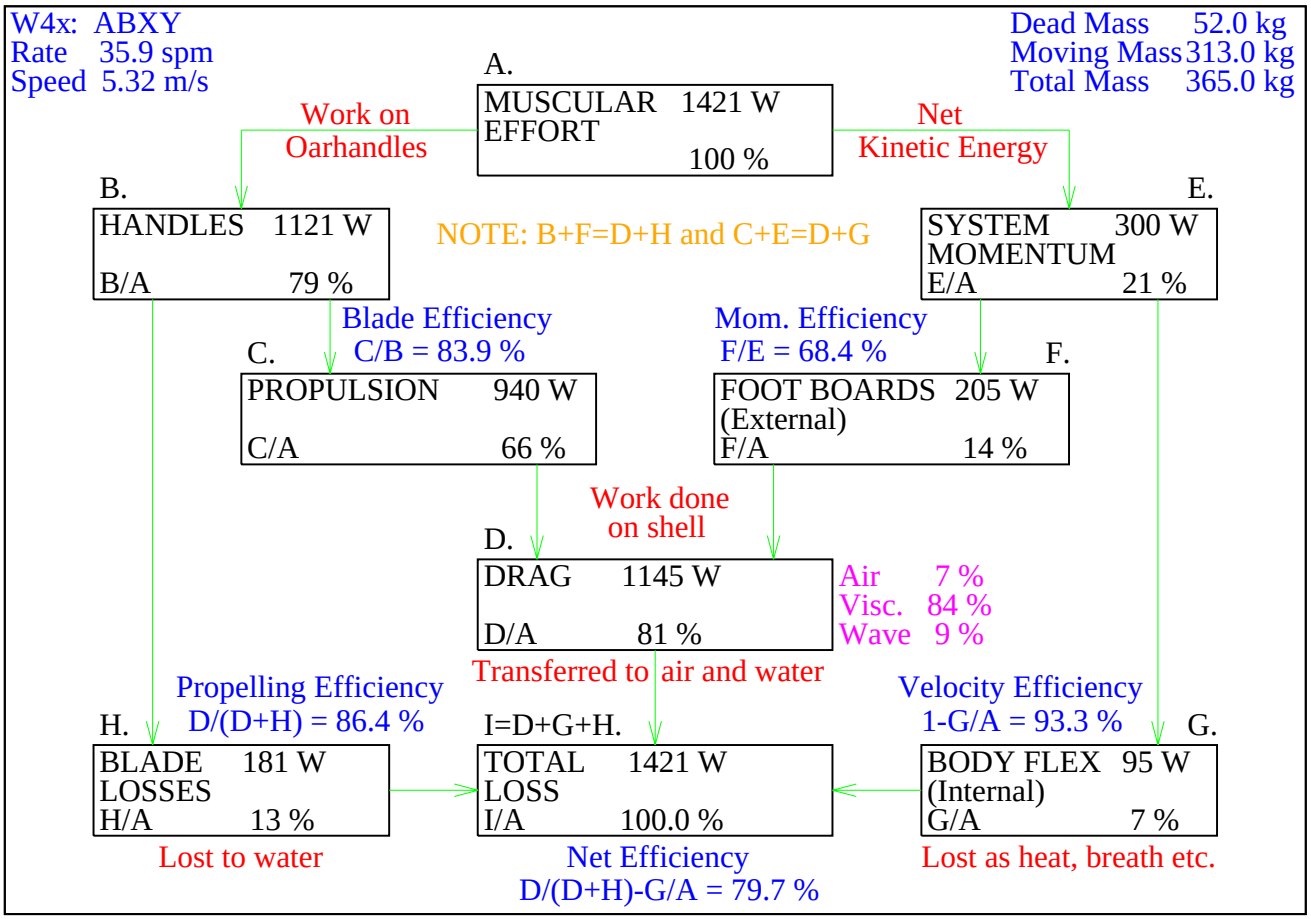

Figure 11: Power flow chart.

1.2 M4x: Men's Quadruple Scull

The on-water trial for this men's quad, "Erdos", "Ganya", "Singh" and "Timbo", was conducted over 2000m on an early autumn morning. Air and water temperatures were not recorded: they were estimated as 10°C and 17°C respectively. Measured values of rigging details, oar angles, gate normal forces, and their anthropometry were used as input to FIRM. Body angle regimes were not recorded but were estimated by the author using a complicated fitting process.

Table 3: Summary of experimental results for this simulation: number of strokes, stroke rate, non-dimensional pull phase duration (t_p/t_s), minimum hull velocity (U_{min}), maximum hull velocity (U_{max}), and mean hull velocity ($\overline{U}$).

Item	Value
Nstrokes	25
Rate (spm)	34.217 ±0.245
t_p/t_s	0.469 ±0.006
U_{min} (ms^{-1})	4.150 ±0.029
U_{max} (ms^{-1})	6.492 ±0.036
$\overline{U}$ (ms^{-1})	5.572 ±0.030

Table 3 summarises the main quantities relating to the simulation for this crew. Values are given ± one standard deviation.

Table 4: Experimental oar-related values for this simulation: Minimum and maximum oar angles, and maximum gate normal force.

Name	Port Oar			Starboard Oar		
	Min. Angle (degrees)	Max. Angle (degrees)	Max. F_{Gn} (N)	Min. Angle (degrees)	Max. Angle (degrees)	Max. F_{Gn} (N)
Erdos	-60.5±0.59	45.6±0.54	595.2±29.4	-61.2±0.48	40.9±0.43	494.2±25.3
Ganya	-57.8±0.51	43.0±0.49	416.2±19.2	-60.2±0.50	44.6±0.91	559.6±24.5
Singh	-63.6±0.48	40.5±0.40	588.8±23.4	-61.4±0.57	43.7±0.48	448.3±20.5
Timbo	-62.0±0.50	38.2±0.40	585.0±26.6	-61.9±0.27	43.1±0.67	458.5±24.9

Table 4 summarises the measured oar angles and gate normal forces for this simulation. Note that the standard deviations of the gate forces are quite high for this crew.

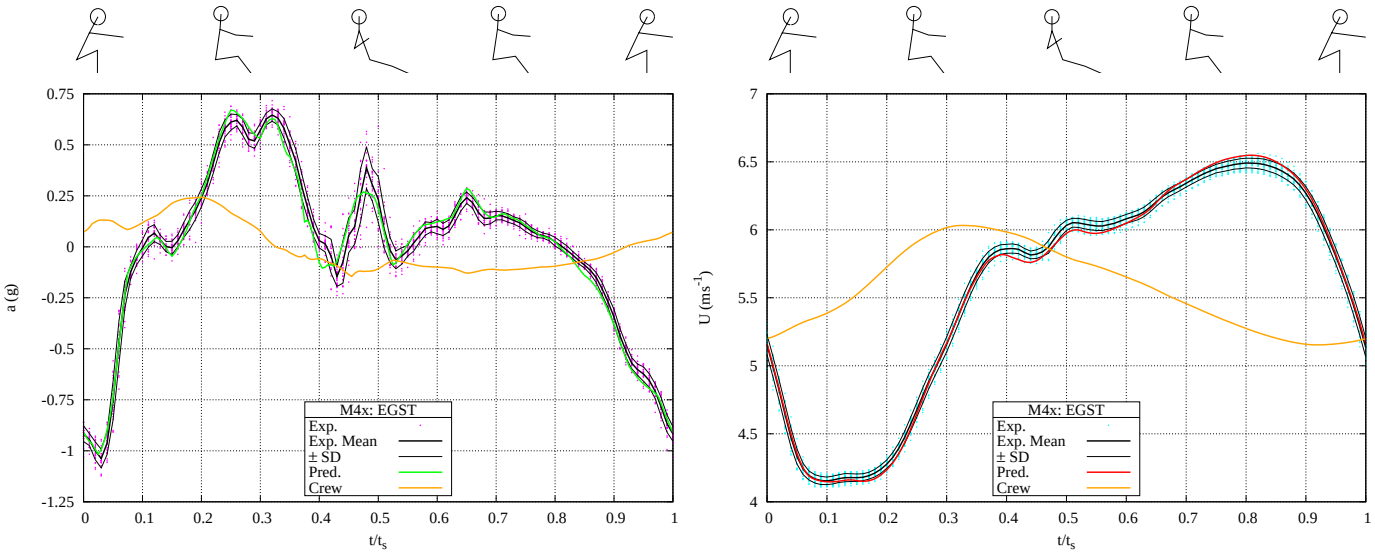

Figure 12: Hull propulsive acceleration and crew cg acceleration (left); hull velocity and crew cg velocity (right).

The hull propulsive acceleration is shown in the left panel of Fig. 12. Experimental data is shown as pink dots; the thick black curve is the mean of the measured values and the thin lines are one standard deviation (SD) either side of the mean curve. The green curve is FIRM's prediction.

Hull propulsive velocity and the speed of the crew CG is shown in the plot at the right of Fig. 12.

The forces in the equations of motion are shown in the left panel of Fig. 13. Drag components during the stroke are in the panel at the right.

Oar angles are shown in the four plots at the left of Fig. 14; gate normal forces are shown in the four plots in the right column. The values represented by the solid curves were used as input to FIRM.

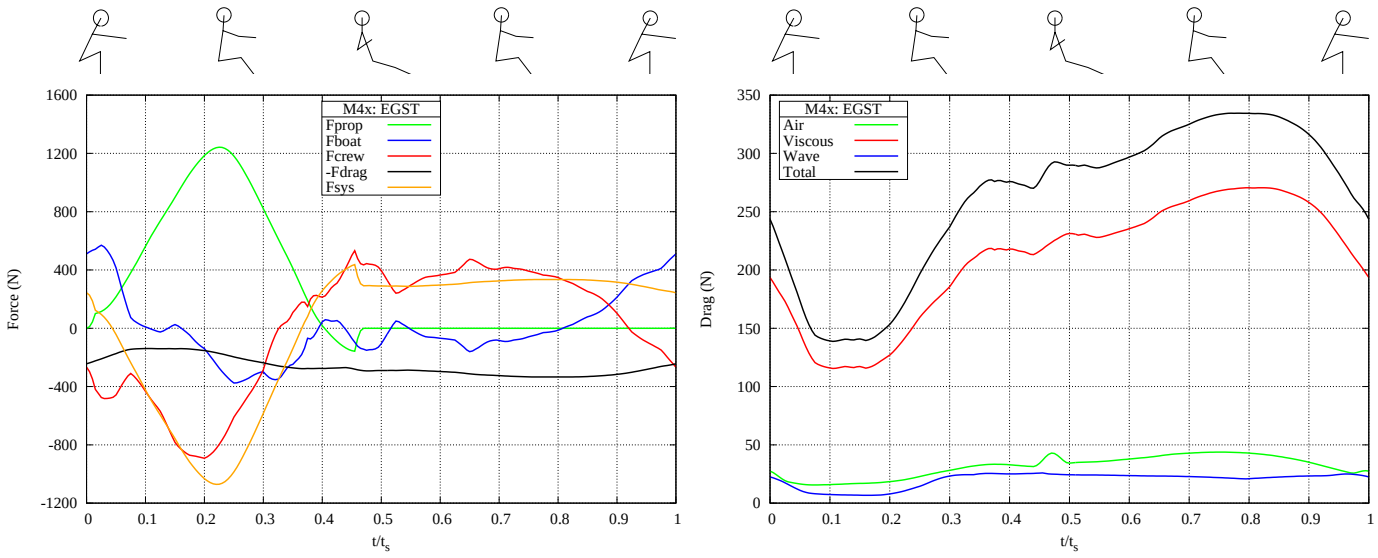

Figure 13: Equation of motion forces (left) and drag components (right).

Blade propulsive forces are shown in the four plots at the left of Fig. 15. Dynamic oar lever ratios shown in the right column of plots in Fig. 15 include the effect of variations in the location of the OBCP during the stroke.

Body angle regimes for two crew members are shown in the two parts of Fig. 16. The angles are the same for both crew members in this simulation. Small differences in hip angles are due to their different feet heights.

Joint trajectories for two crew members are shown in the two parts of Fig. 17. Small differences between the two crew members are due to their different limb lengths.

CG trajectories for two crew members are shown in the two parts of Fig. 18. Small differences between the two crew members are due to their different limb lengths.

Yawing moment lever arms and yawing moments are shown in the two parts of Fig. 19.

The OBCP trajectories in the yz-plane are shown in Fig. 20. For the purposes of this plot, the OBCP is assumed to be at the geometric centre of the blade when it is out of the water.

The OBCP is below the water from about $t/t_s = 0.01$ to $t/t_s \approx 0.47$. The latter value is the value entered in the main input file.

The OBCP trajectories in Fig. 21 have been plotted on the same side of the hull for clarity and comparison.

The OHCE x-wise velocities are shown in Fig. 22.

The x-wise seat velocities are shown in Fig. 23.

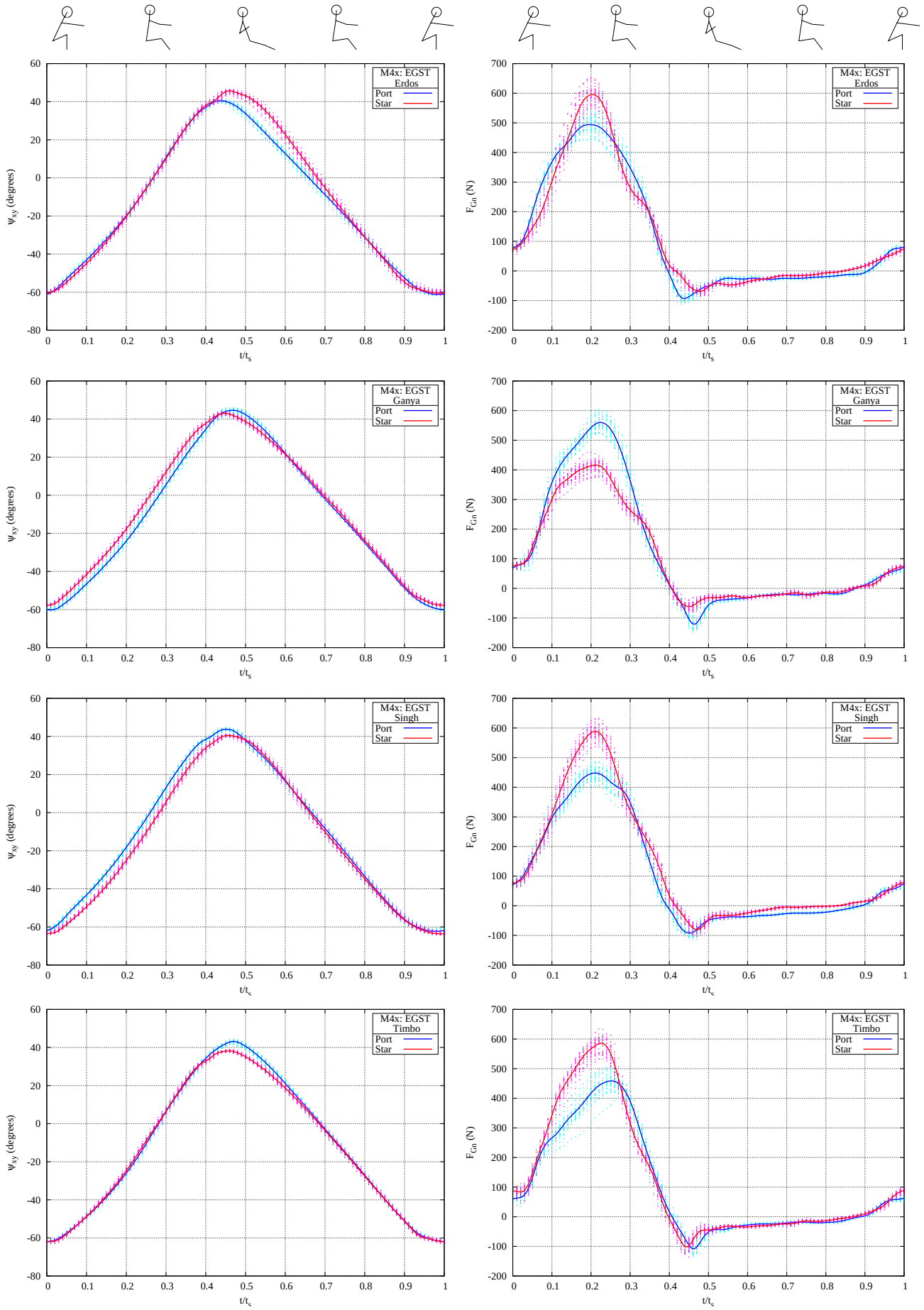

Figure 14: Oar azimuth angles Ψ_{xy} (left column) and gate normal forces F_{Gn} (right). Seat 1 (top row); Seat 2 (second row); Seat 3 (third row) and Seat 4 (bottom row).

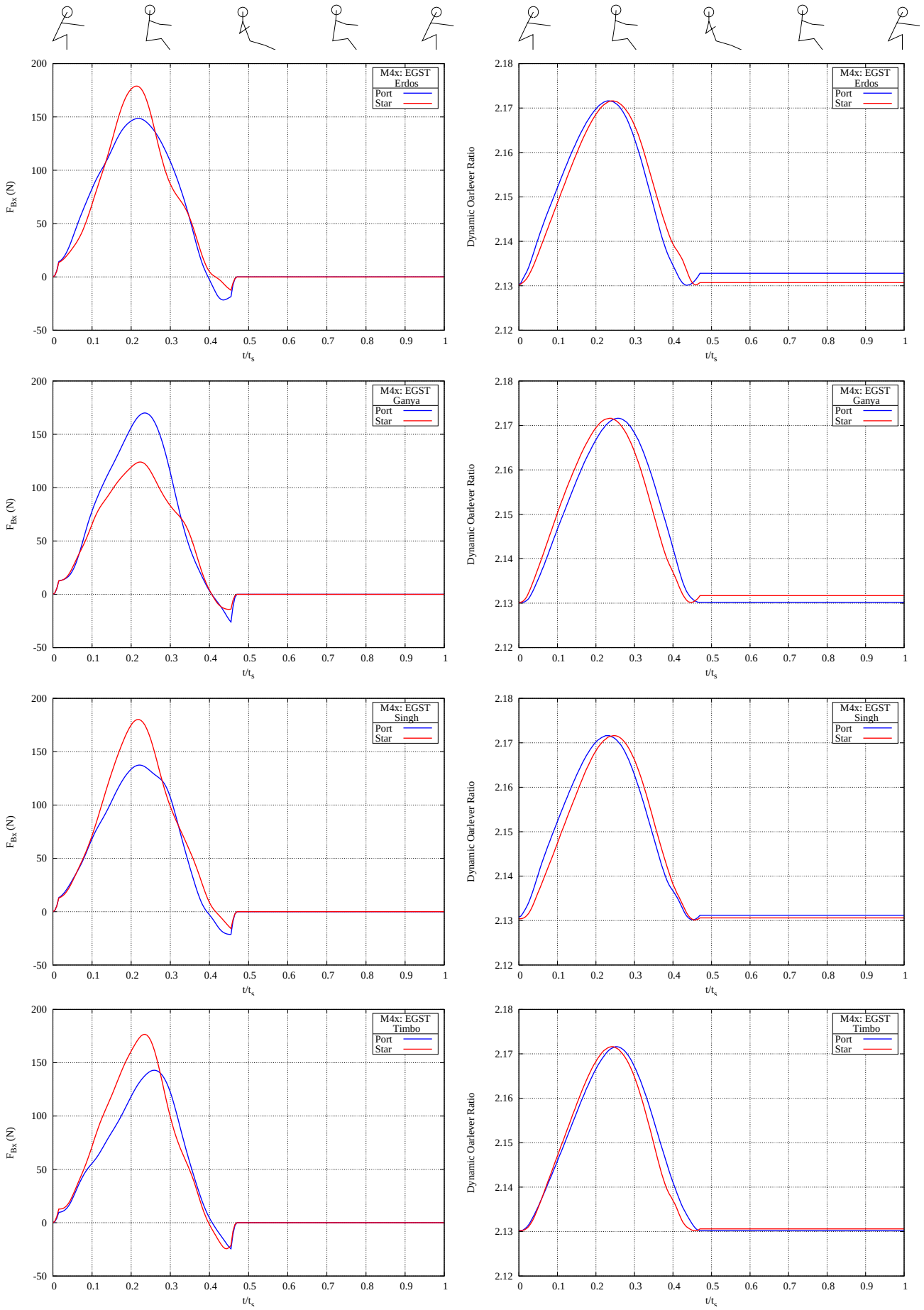

Figure 15: Blade propulsive forces F_{Bx} (left column) and dynamic oar lever ratios (right). Seat 1 (top row); Seat 2 (second row); Seat 3 (third row) and Seat 4 (bottom row).

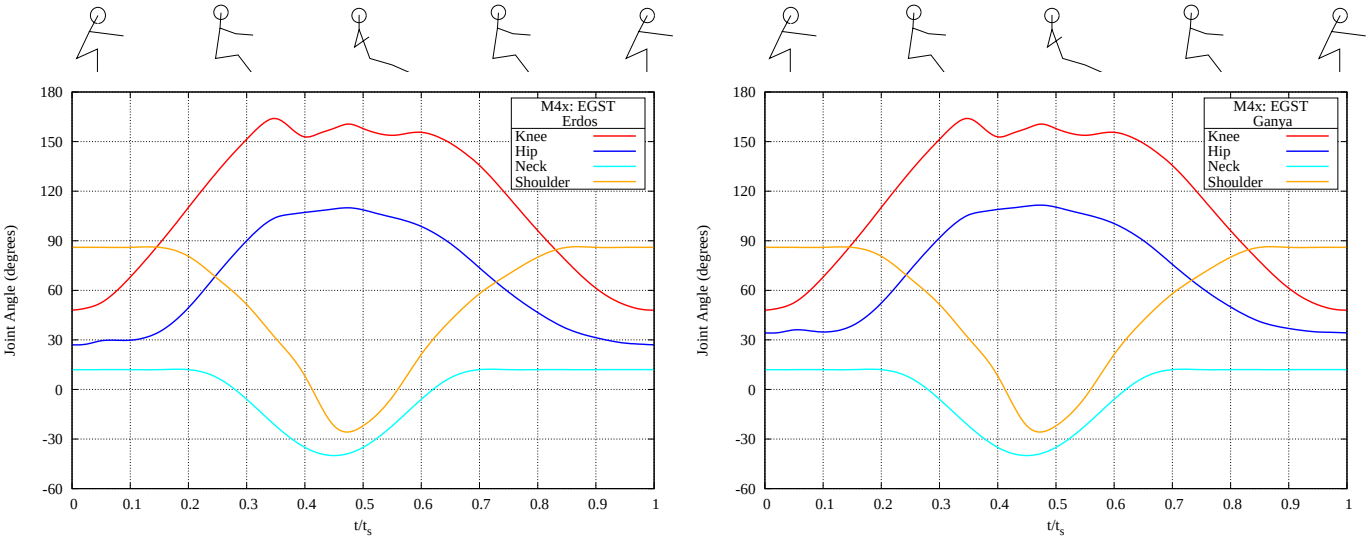

Figure 16: Joint angles: Seat 1 (left): Seat 2 (right).

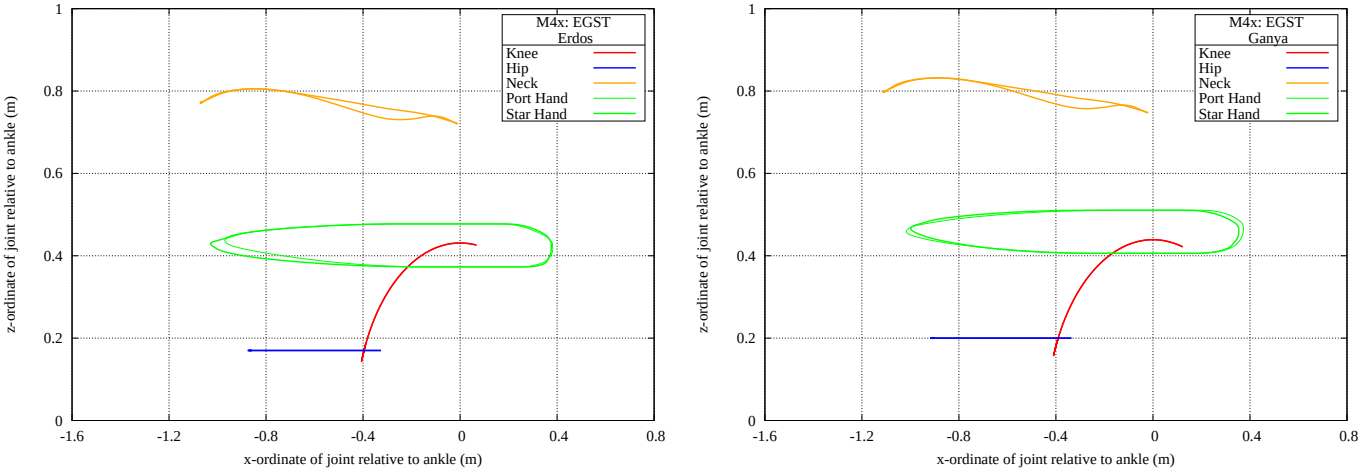

Figure 17: Joint trajectories: Seat 1 (left): Seat 2 (right).

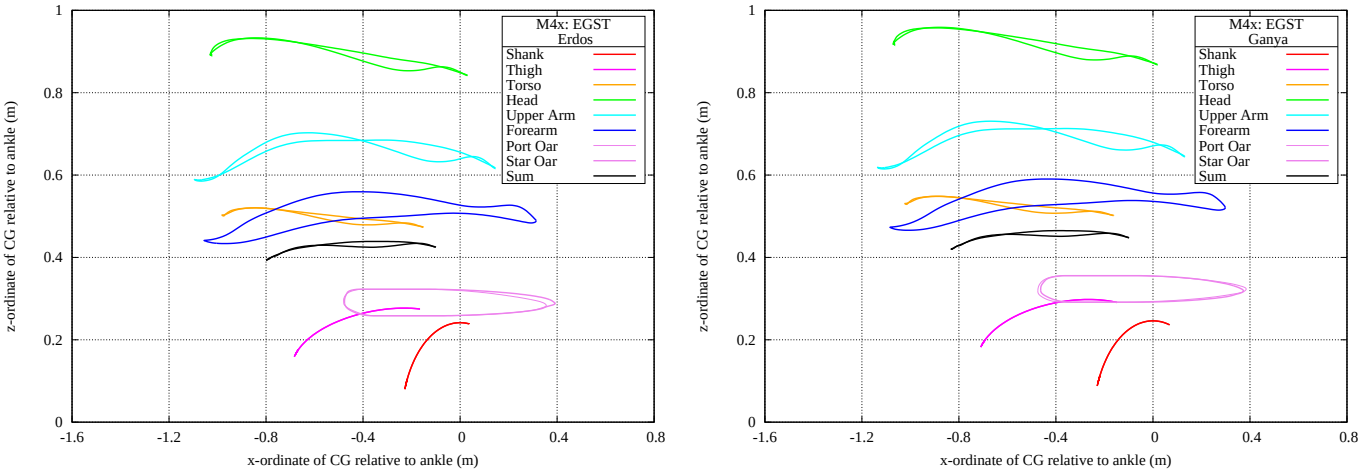

Figure 18: Trajectories of body part centres of gravity: Seat 1 (left): Seat 2 (right).

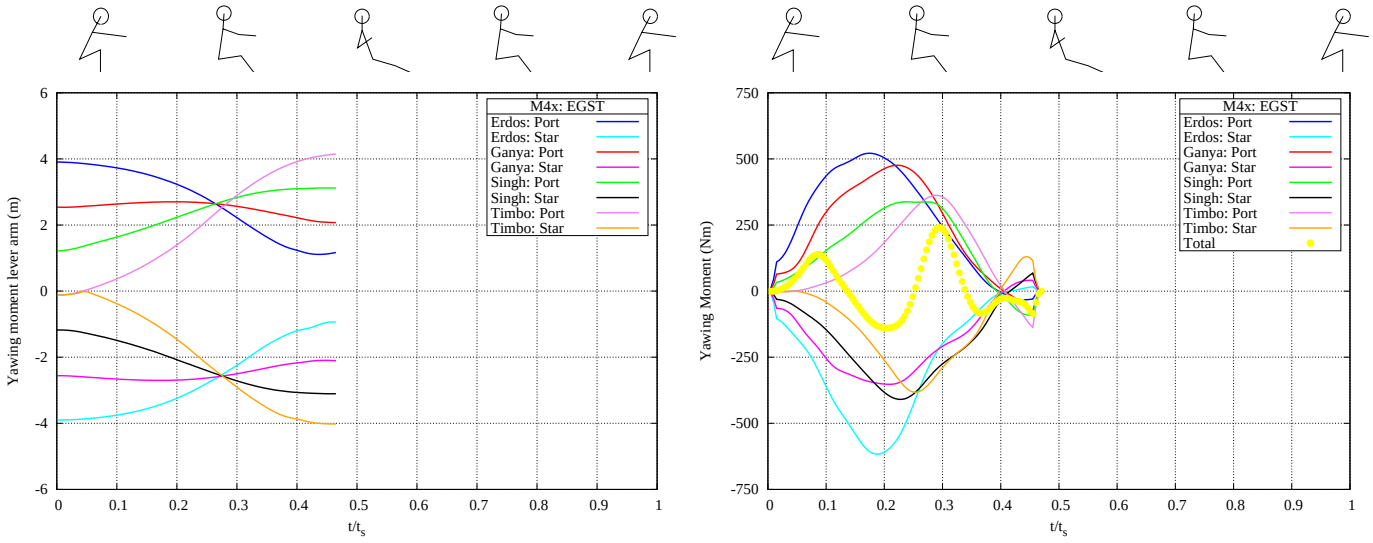

Figure 19: Yawing moment lever arms L_{yaw} (left); yawing moments M_{yaw} (right).

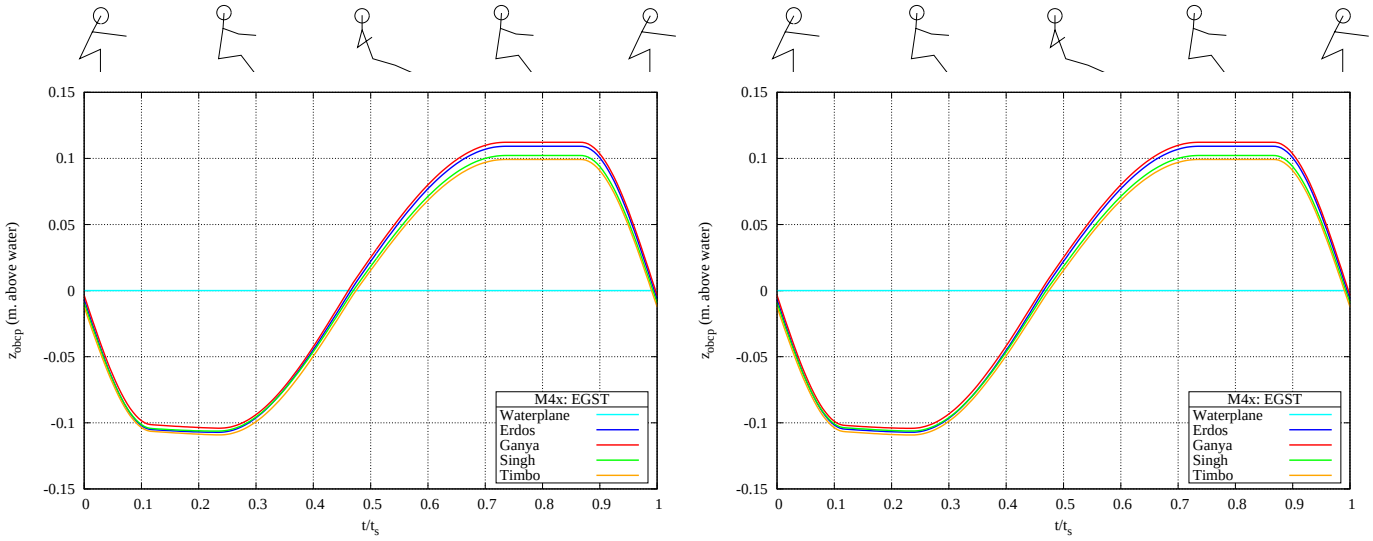

Figure 20: OBCP trajectories in the yz-plane: Port side (left); Starboard side (right).

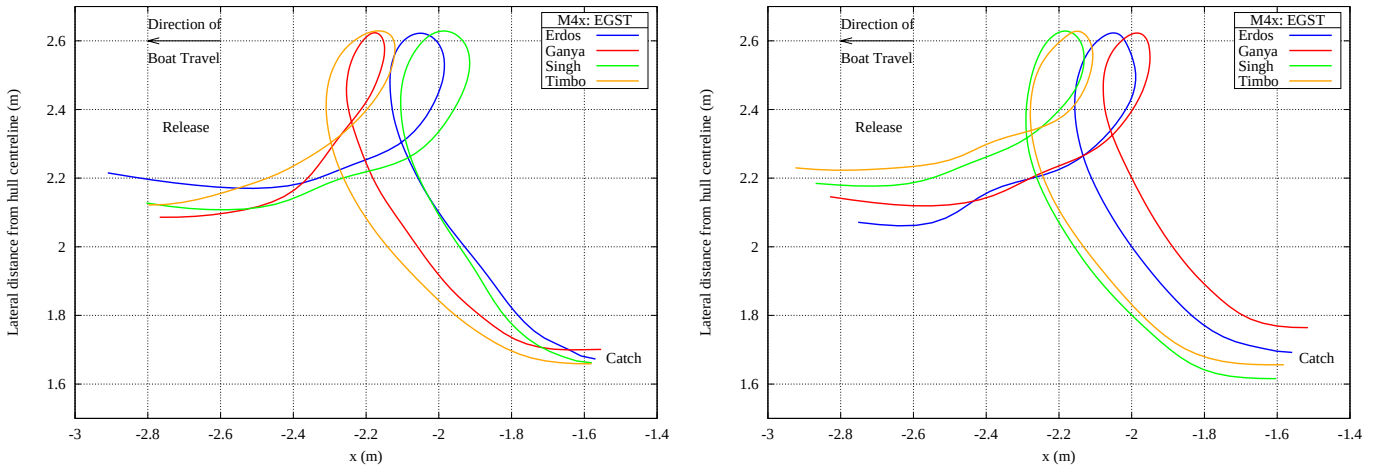

Figure 21: OBCP trajectories in the xy-plane: Port side (left); Starboard side (right).

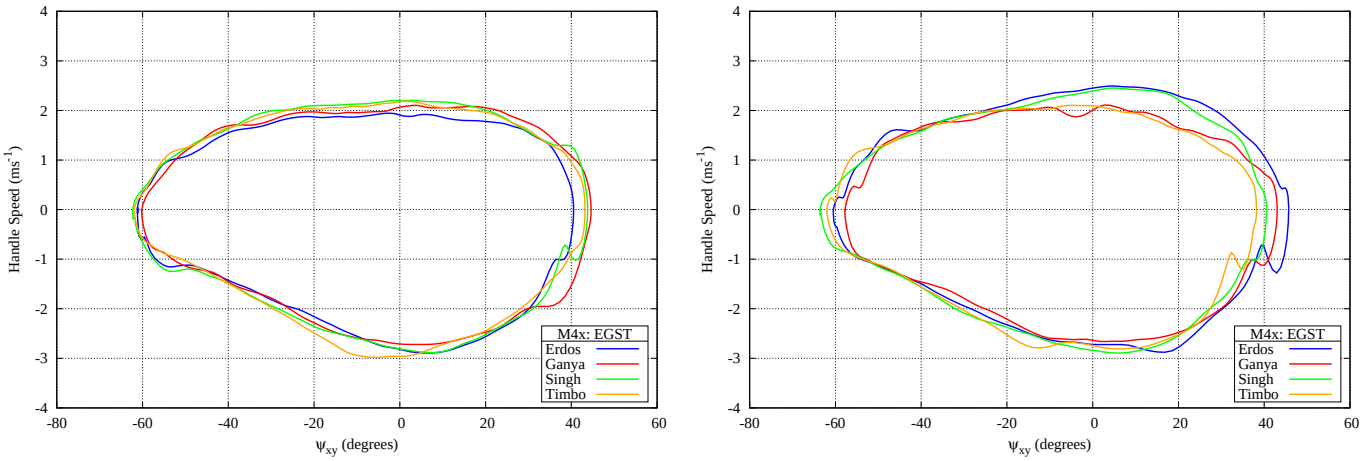

Figure 22: OHCE x-wise velocity: Port side (left); Starboard side (right).

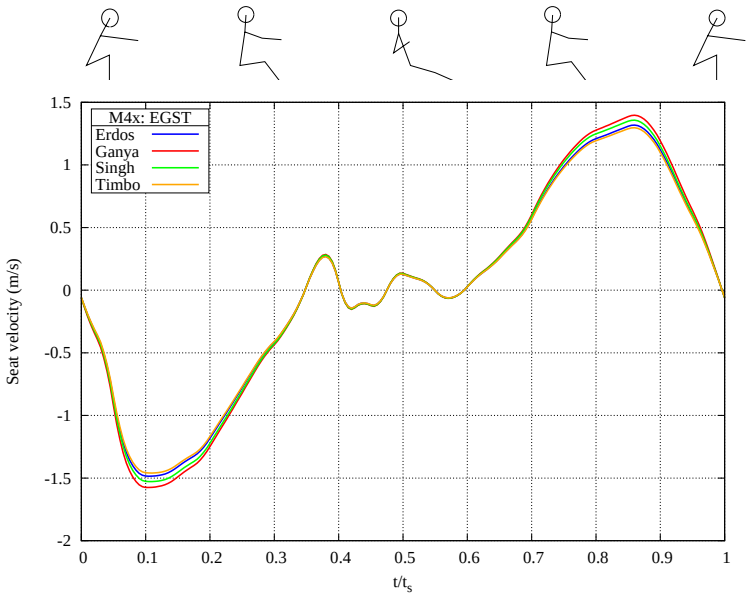

Figure 23: Seat x-wise velocities.

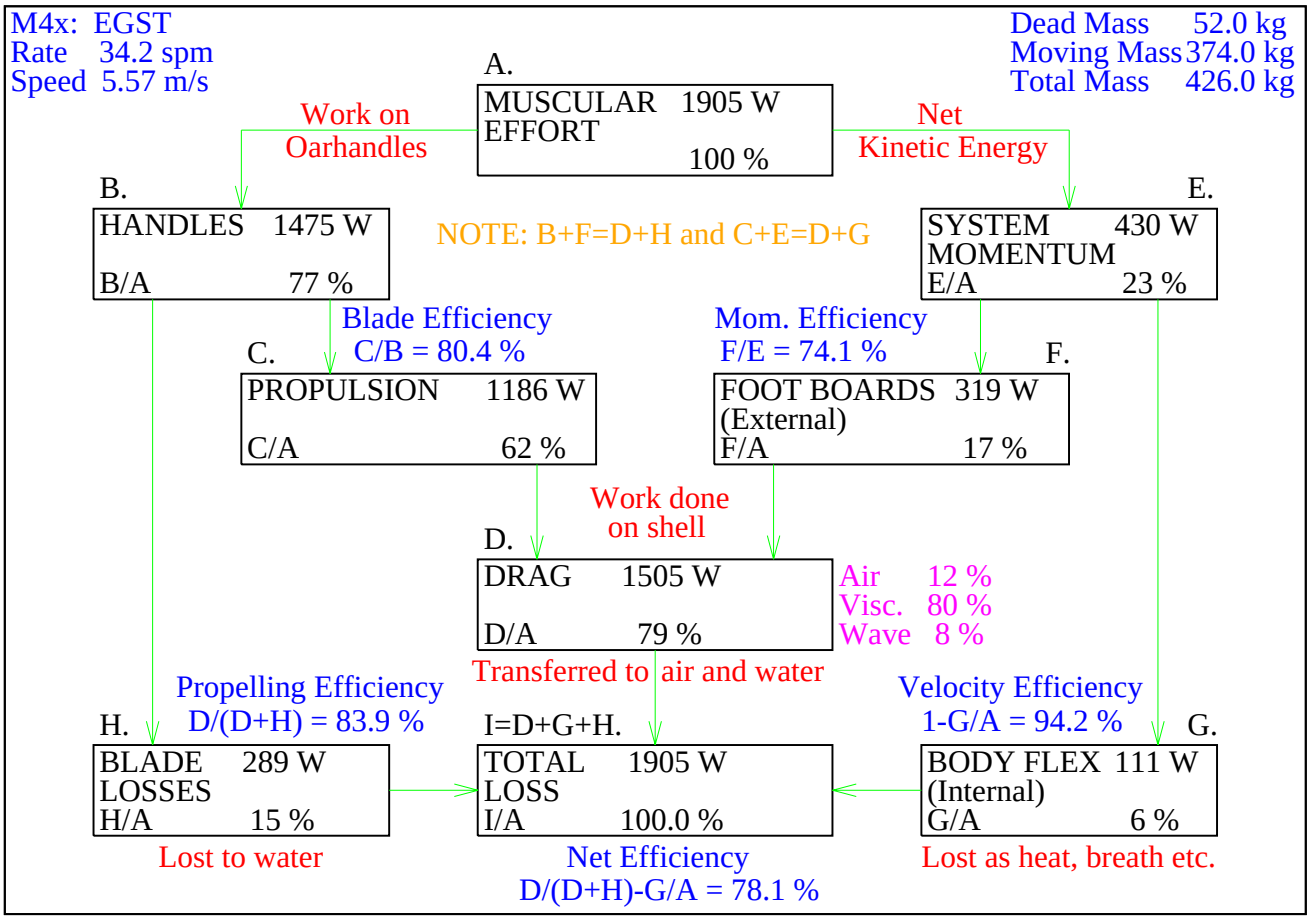

Figure 24: Power flow chart.